JOURNAL OF KUFA–PHYSICS
journal.uokufa.edu.iq/index.php/jkp/index | ISSN: 2077–5830

Improving the Coating Properties of Petroleum Product Pipelines Using Nanomaterials

Fadhil K. Farhan[1], Zainab F. Nazal[2]*, Atheer M. Jameel[3], May A. Abdul Galil[4]

[1,2]*Al-Kharkh University of Science - College of Science - Department of Medical Physics*
[3,4]*Ministry of Industry and Minerals – Iraq- Baghdad*

[*]*Corresponding Author E-mail:* : Zainab.f.n.2022@kus.edu.iq

ARTICLE INF.

Article history:
Received: 3 JUL., 2025
Revised: 1 NOV., 2025
Accepted: 24 NOV., 2025
Available Online: 27 DEC. 2025

Keywords:

AL_2O_3
Composites
Coating
Corrosion
Tafel method

ABSTRACT

In this research, coating mixtures of several percentages were prepared using aluminium oxide or alumina powder AL_2O_3. Pieces of petroleum derivatives pipes were selected and formed with equal dimensions (2x2x2) mm with a number of (5) pieces. The mixtures were prepared using the liquid mixing method and ultrasonic technology to stimulate the composites (coatings) from a percentage of (5%) to a percentage of (20%) of (AL_2O_3). Then they were mixed and added to the paint used in coating the pipes by immersion. The Tafel method was used to calculate the corrosion rate (electrochemical method) and the soil immersion method, and the results were compared between the two methods. The results showed a significant improvement for the samples reinforced with a percentage of (10%), the lowest corrosion rate, compared to the pure model and the coated model free of additives and the rest of the percentages.

DOI: https://doi.org/10.31257/2018/JKP/2025/v17.i02.20260

تحسين خصائص طلاء خطوط أنابيب المنتجات البترولية باستخدام المواد النانوية

فاضل كريم فرحان[1] ، زينب فالح نزال[2] ،
اثير محمد جميل[3]، مي عبد الله[4]

[1,2]جامعة الكرخ للعلوم-كلية العلوم-قسم الفيزياء الطبية
[3,4]وزارة الصناعة والمعادن-العراق-بغداد

الـــخُـــلاصـــة

في هذا البحث، تم تحضير مخاليط طلاء من عدة نسب مئوية باستخدام أكسيد الألومنيوم أو مسحوق الألومينا. تم اختيار قطع أنابيب المشتقات البترولية وتشكيلها بأبعاد متساوية (2 * 2 * 2) مم بعدد (5) قطع. تم تحضير المخاليط باستخدام طريقة الخلط السائل وتقنية الموجات فوق الصوتية لتحفيز المركبات (الطلاءات) من نسبة (5٪) إلى نسبة (20٪) من (الألومينا) تم خلطها وإضافتها إلى الطلاء المستخدم في طلاء الأنابيب عن طريق الغمر. تم استخدام طريقة تافل لحساب معدل التآكل (الطريقة الكهروكيميائية) وطريقة غمر التربة، وتمت مقارنة النتائج بين الطريقتين. وأظهرت النتائج تحسنا

الكلمات المفتاحية:

الألومينا
المركبات
الطلاء
التآكل
طريقة تافل.

ملحوظا للعينات المعززة بنسبة (10%) أدنى معدل تآكل مقارنة بالنموذج النقي والنموذج المطلي الخالي من الإضافات وباقي النسب المئوية.

1. INTRODUCTION

In the petroleum industry, corrosion-induced pipeline damage is a common phenomenon mainly affecting transmission pipelines that are buried or underwater. This is considered one of the largest engineering challenges around, and a major economic issue. These challenges emphasize that corrosion-related failures were particularly a concern on the projects [1, 2]. Carbon steels are extensively used in Marin applications, with global production reaching approximately 1.8 billion tons in 2018 [3]. Despite their low corrosion resistance, these materials are employed in various sectors, including those used in marine, transportation, petroleum production and refinement, chemical extraction, nuclear and power plants that burn fossil fuels pipeline construction, mining and metalworking machinery [4]. Due to the environmental and climate variations in Iraq, there are numerous areas likely to be exposed to corrosion. Corrosion problem significantly impacts initiatives, including countless kilometers of pipelines that transport hydrocarbons fractions, petrol, and gas from natural sources in addition to additional underground storage tanks [5, 6]. Corrosion is the process of eroding or degradation metal. This causes a common example of rusting that will cover the steel. The vast majority of corrosion is electrochemical in nature and involves at least two surface reactions taking place on the metal undergoing corrosion. One of these reactions is oxidation (corrosion) which results in dissolving away iron, and it is also called anodic reaction. The second is a response of reduction. (e.g. oxygen) and it is called partially cathodic interaction. The outcomes of the electrochemical processes are chemically compatible to combining each other in a non-electrochemical reaction (e.g., rust) [7]. Generally, corrosion is the process of performance deterioration in metals due to medium effected surrounding area [8,9]. There are two primary concerns seen in the progressive and regressive Oil and Gas sectors. External and internal corrosion are related to hydrocarbons delivering pipeline system. The first one is a sort of damage that is usually caused by water intrusions saturated with aggressions ions as the major variance affects corrosion surfaces. Mechanical failure may be initiated by any number of things including water solution [10–11]. It may prove to be to somewhat important in the overall outcome that the difference in tension, form, and harm might never be managed by the outer or inward pressure exerted on pipelines. The outside and inward erosion procedures have adverse effects. Therefore, the summed up (uniform) and confined consumption harm potentially are credited to pressure erosion breaking (stress corrosion cracking) [12-13]. The ceramic components such as SnS, SnS_2 TiO_2 and Al_2O_3 are utilized in the coating. It is appropriate when using the thermal spray technique [14, 15, 16, and 17]. TiO_2 has excellent ear resistance and thus enhancing the mechanical qualities

of the coating, while TiO_2 is chemically inactive and has a high degree of arm solidity. Two ceramic materials that are frequently used for erosion assurance coatings are titania (TiO_2) and alumina (Al_2O_3). The towering hardness of Al_2O_3 is well known. The primary protection against corrosion for an underground pipeline is coatings. The second line of defense against corrosion is cathodic protection (CP), notwithstanding its application.[19]. Because of the wide variety of needs and uses within various sectors, coating techniques come in a large variety. These procedures provide a variety of material microstructure outcomes, efficacy, suitability, and resilience while incorporating a large number of various online and offline parameters. Based on the intended performance, coating methods can be useful in some situations, with corrosion and ear protection, being the most crucial [20]. The use of pipelines for a variety of applications is always connected to the environment, including soil, water, and air. Temperature, relative humidity, ion concentration, and solution resistance all affect how corrosive each of these conditions is. For instance, the solution's NaCl content varies [21]. The proficiency of consumption procedures to the ASTM guidelines as shown by the Tafel test relied upon the kind of the electron source and electrode anodes, Moreover, when electrolyte arrangement is fixed, electricity changes [22]. Point of current review will be used to test erosion conduct of Alumina The addition of nanoparticles to coating material soil fixations is succeeded by utilizing Polarization of Tafel technique.

2. METHODS AND MATERIALS

We received Pipe made of carbon steel (A 106) from the Iraqi Ministry of Industry. Soil was provided from a site near the Shuaiba refinery in Basra Governorate. Table (1) demonstrates the as-received (CS) chemical composition. Figure (1) shows samples of α-Al_2O_3 nanoparticles that were synthesized via the sol-gel method. 150 ml of pure water was used for fully dissolving 10 g of Al $(NO_3)_3 \cdot 9H_2O$, producing an amount of 0.18 M. Weight of the materials was assessed using a delicate electronic balancing device (Gen ex Laboratories) with accuracy of four digits. A thorough mixing of the solution was done with a magnetic stirrer at room temperature and (14) milliliters of an ethanol solution were then added, drop by drop. The solution's temperature was progressively increased to 80°C. The solution has a pH range of two to three. For 40-45 minutes, the solution was maintained in the magnetic stirrer container was gradually evaporated forming the sol-gel solution. The product was dried in an oven for three hours at 80°C and cooled in the room temperature to obtain a dry white powder. A sieve of (200 x 50) mm and 75 μm in diameter was used to filter the powder after it had been ground into an incredibly fine powder. [23]. Figure (2) shows twelve samples of (2x2x2) mm that were manufactured and divided into two groups. Each group contains six samples (pure, normal coating without additives, coating with 5% AL_2O_3 added, coating with 10% AL_2O_3 added, coating with 15% AL_2O_3 added, coating with 20% AL_2O_3 added) and subjected

to an electrochemical reaction. The second group was buried under the soil for three months. The samples of the first group were immersed in a solution of raw water mixed with soil at a rate of 3.5% per (1) L. Prior to being polished in accordance with the process of metallography, the specimens were washed with ethanol. Various Sic abrasive sheets (400, 600, 800, 1000 and 1200 Sic grits/in^2) were used to polish the samples. The corrosion cell utilized in this study was composed of three electrodes and had a volume of one liter. The first group's electrochemical test was conducted at room temperature using samples that had been fixed in the raw water mix soil at a concentration of 3.5%. Using a magnetic stirring device, 35 grams of soil and 1000 milliliters of raw water were mixed to create a corrosion solution, which was then allowed to sit at ambient temperature for 10 minutes. 1000 milliliters of a 3.5% soil solution were used to submerge the steel specimens. The following formula was used to calculate the corrosion rate (C_R) [24]:

$$\text{Corrosion rate} = \text{i corr}\ \frac{\text{K(EW)}}{\text{A}\ .\rho}$$

where C_R is corrosion rate, expressed in units, which is based on the value of K. For mild steel, i_{corr} is the corrosion current in amperes, A is the sample area in cm^2, EW is the density of the sample metal by equivalent weight (27.92 g/equivalent), ρ is the density of the sample material in gram per cm^3 (7.87), and K is a value used to specify the units of the oxidation rate (1.288 × 105) for mpy units [24]. The weights of the second group samples were measured before and after burial.

Figure (1) sample of AL_2O_3

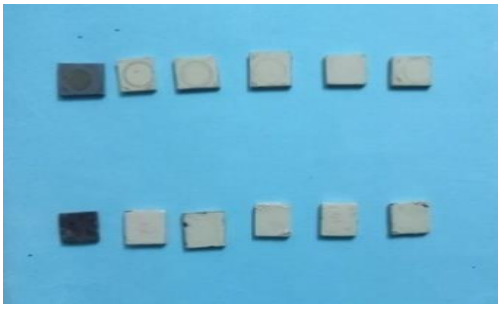

Figure (2) Twelve models

3 . RESULTS AND DISCUSSION

Figure (1) show patterns of XRD diffraction of synthetic (AL_2O_3) tiny particles which were made by (sol-gel) method. The peak with the highest intensity is at 57.26°. Scherer's equation, which is based on the (FWHM) of the many highest intensities at values for variables, was used to determine the diameter of the nanoparticles [25]:

$$A = 0.94\ \lambda\beta\ cos\theta$$

Where A is sizes of particles, the full width at half maximum of the scattering peak, X-ray radiation's wavelength is λ, θ indicates diffraction degree. The Scherrer size of the NPs is generally (38.75) nanometer.

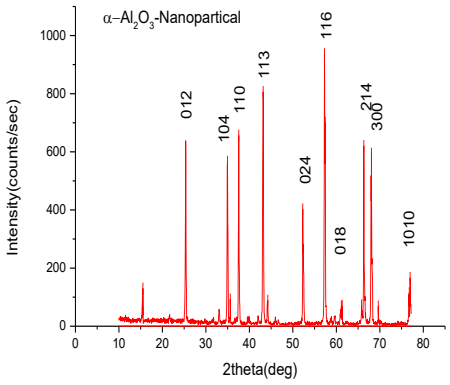

Figure (3) show XRD diffraction patterns

A procedure for chemical analysis [26] was carried out to determine materials' composition of the twelve models is shown in tables (1,2,3,4,5,6,7,8,9,10,11 and 12). Elements and percentages of the steel used are listed.

Table -1- Chemical component of CS A 106 Pure

Elements	C	Mn	Si	Al	P	S	Cr	Ni	Mo	V	Cu	Fe
Value %	0.23	0.76	0.0400	0.011	0.017	0.019	0.32	0.19	0.08	0.04	0.24	Remaining

Table -2- chemical component of CS coating 0% Al_2O_3 (electrochemical).

Elements	C	Mn	Si	Al	P	S	Cr	Ni	Mo	V	Cu	Fe
Value %	0.23	0.38	0.0033	0.0096	0.021	0.0027	0.12	0.04	0.126	0.02	0.149	Remaining

Table -3- Chemical component of CS coating 0% Al_2O_3 (under soil).

Elements	C	Mn	Si	Al	P	S	Cr	Ni	Mo	V	Cu	Fe
Value %	0.23	0.634	0.0032	0.0097	0.0071	0.0046	0.093	0.005	0.075	0.019	0.044	Remaining

Table -4- Chemical component of carbon steel coating with 5% Al_2O_3 (electrochemical).

Elements	C	Mn	Si	Al	P	S	Cr	Ni	Mo	V	Cu	Fe
Value %	0.23	0.228	0.0025	0.0073	0.0387	0.0039	0.073	0.054	0.168	0.073	0.0504	Remaining

Table -5 - Chemical component of CS coating with 5% Al_2O_3 (under soil).

Elements	C	Mn	Si	Al	P	S	Cr	Ni	Mo	V	Cu	Fe
Value %	0.23	0.351	0.0383	0.0077	0.0232	0.0053	0.083	0.0357	0.128	0.024	0.0528	Remaining

Table -6 - Chemical component of CS coating with 10% Al_2O_3 (electrochemical).

El	C	Mn	Si	Al	P	S	Cr	Ni	Mo	V	Cu	Fe

ements												
Value%	0.23	0.2322	0.009229	0.0077	0.0614	0.0055	0.099	0.0288	0.148	0.029	0.0337	Remaining

Table -7- Chemical component of CS coating with 10% Al_2O_3 (under soil).

Elements	C	Mn	Si	Al	P	S	Cr	Ni	Mo	V	Cu	Fe
Value%	0.23	0.328	0.089	0.391	0.0479	0.0020	0.088	0.0380	0.257	0.020	0.0298	Remaining

Table -8 - Chemical component of CS coating with 15% Al_2O_3 (electrochemical).

lements		n	i	l			r	i	o		u	e
Value%	.23	.173	.0025	.0074	.0534	.0051	.057	.0463	.145	.033	.0380	emaining

Table -9- Chemical component of CS coating with 15% Al_2O_3 (under soil).

lements		n	i	l			r	i	o		u	e
Value%	.23	.364	.0271	.0159	.0231	.0101	.099	.0340	.145	.022	.0557	emaining

Table -10- Chemical component of CS coating with 20% Al_2O_3 (electrochemical).

Elements	C	Mn	Si	Al	P	S	Cr	Ni	Mo	V	Cu	Fe
Value%	0.23	0.112	0.0027	0.0063	0.0496	0.0034	0.091	0.0813	0.185	0.034	0.0372	Remaining

Table -11- Chemical component of CS coating with 20% Al_2O_3 (under soil).

Elements	C	Mn	Si	Al	P	S	Cr	Ni	Mo	V	Cu	Fe
Value%	0.23	0.1225	0.112	0.0060	0.00730	0.00020	0.0317	0.07001	0.224	0.032	0.0034	Remaining

- Figures,2,3,4,5,6,7,8,9,10,11,12 and 13 show the optical microscope examination of the 6 samples exposed to electrochemical reaction and shows the effect and effectiveness of the (Al_2O_3) material, which gave the coating surface higher corrosion resistance and hardness at a ratio of 10%. Also, for the 6 samples exposed to burial, the lowest mass loss appears at a ratio of 10%, as in Figure 13 which shows, the effect of the nanomaterial on the coating surface and its high resistance to soil reaction.

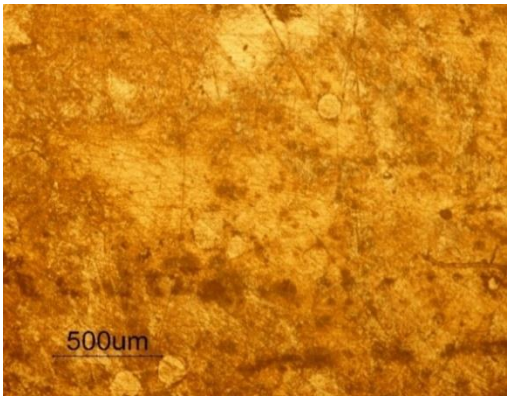

Figure (4) for pure before electrochemical reaction

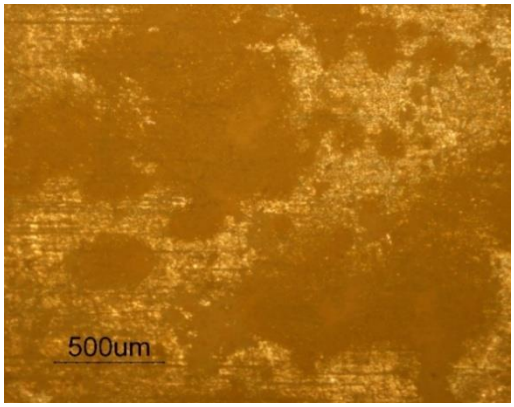

Figure (5) for pure after electrochemical

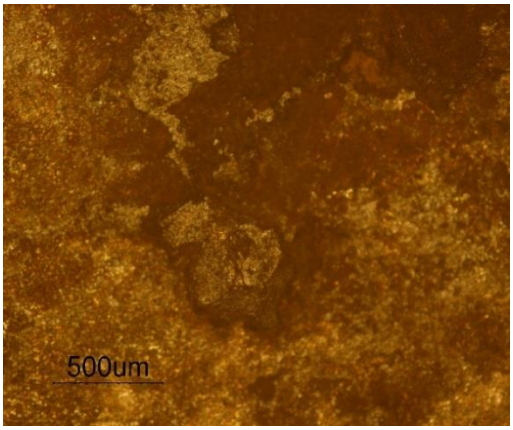

Figure (6) for pure after under soil

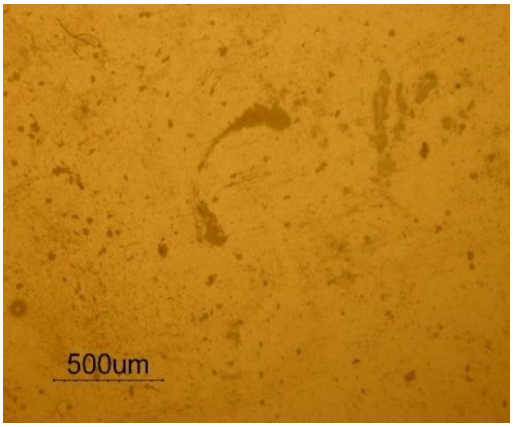

Figure (7) for coating 0% electrochemical reaction

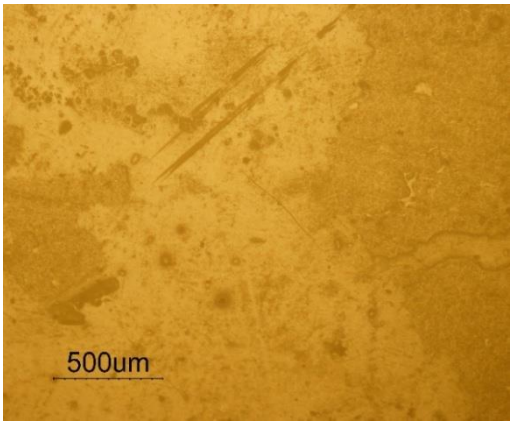

Figure (8) for coating 0% under soil

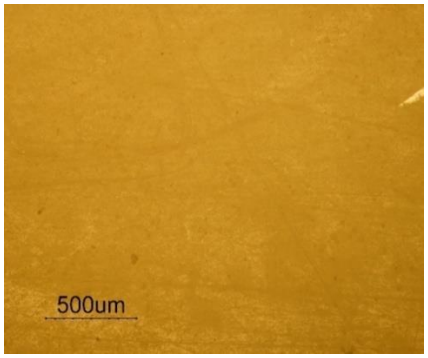

Figure (9) for coating 5% AL_2O_3

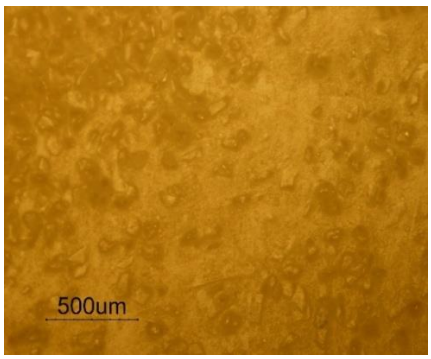

Figure (10) for coating 5% AL_2O_3 under soil Electrochemical reaction

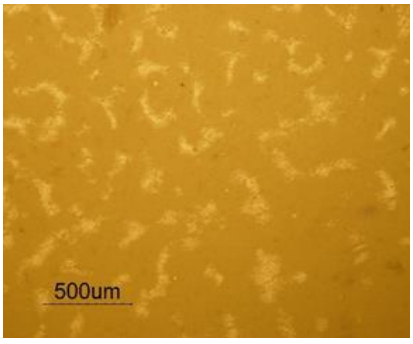

Figure (11) for coating 10 % AL_2O_3

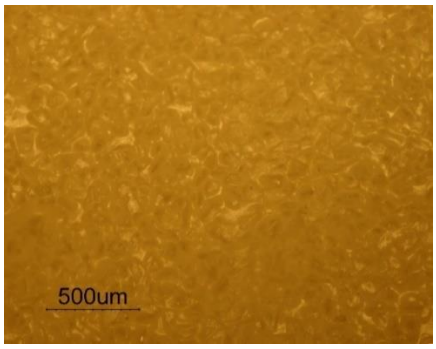

Figure (12) for coating 10 % AL_2O_3 under soil electrochemical reaction

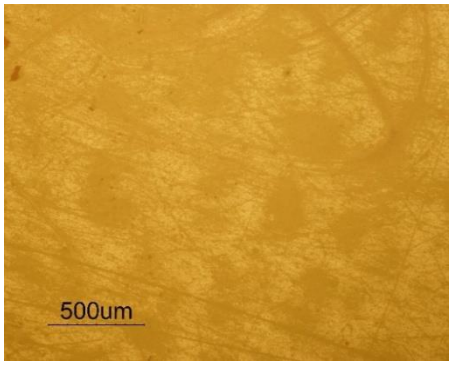

Figure (13) for coating 15 % AL_2O_3

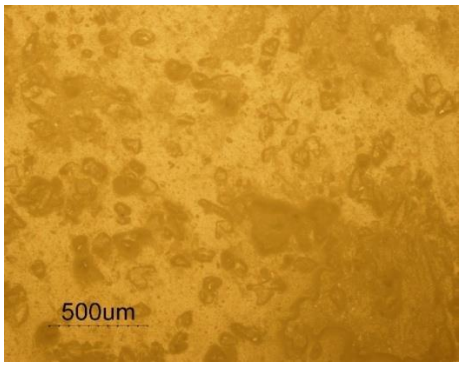

Figure (14) for coating 15 % AL_2O_3 under soil Electrochemical reaction

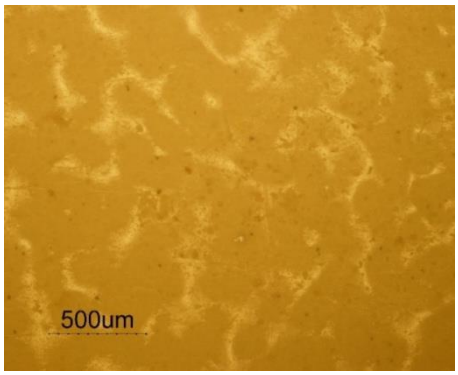

Figure (15) for coating 20 % AL_2O_3

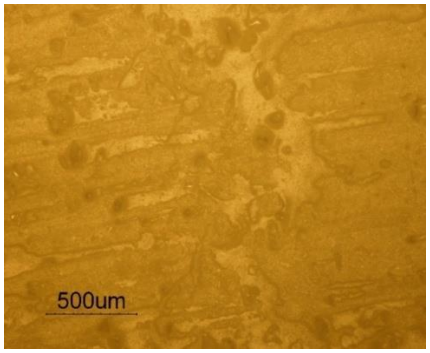

Figure (16) for coating 20 % AL_2O_3 under soil electrochemical reaction

Before the electrochemical experiments were performed, open circuit potentials (OCP) were measured in the electrolyte. After 30 minutes of electrolyte submerging, the samples were measured for (OCP) for 30 minutes. The polarizing graphs of potentiodynamics of the specimens are illustrated in Figure 15,16,17,18,19 and 20. By scanning the starting current from a negative value (-10 mA) to a final positive value (+10 mA) at a scan rate of 0.167 mA/s, the polarization was created. According to the polarization curves, (E_{corr}) of the specimens 10% was comparatively better than the (E_{corr}) of the specimens with (pure,0%,5%,15%,20%).

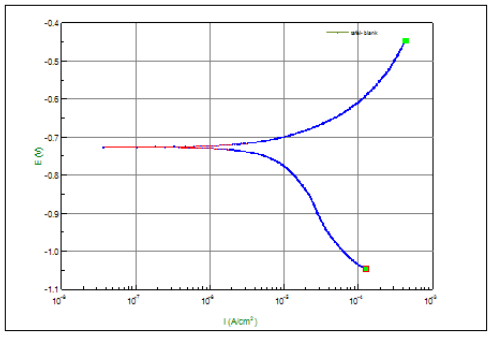

Figure (17) Tafel curve of pure models

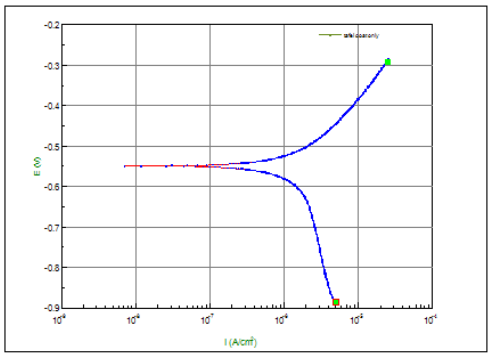

Figure (18) Tafel curve of coating 0% AL_2O_3

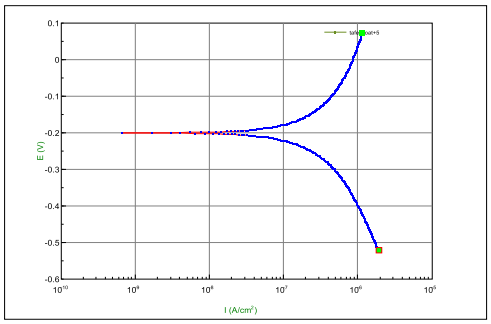

Figure (19) tafel curve of coating 5% AL_2O_3

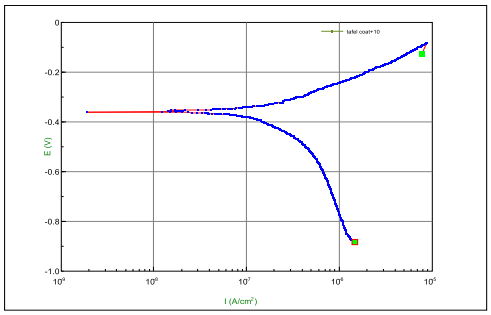

Figure (20) tafel curve of coating 10% AL_2O_3

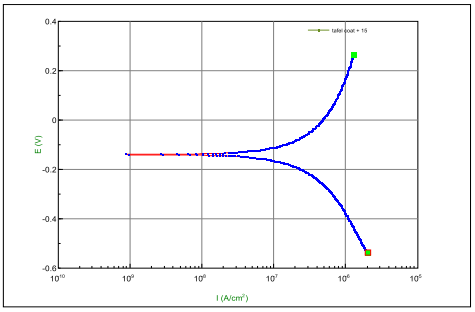

Figure (21) tafel curve of coating 15% AL_2O_3

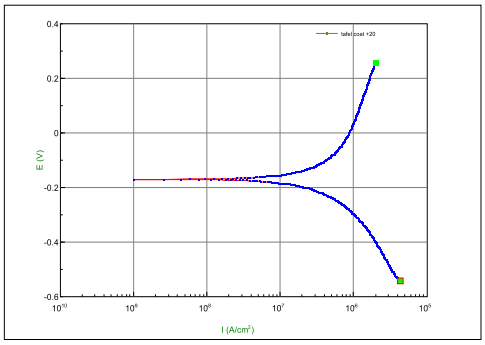

Figure (22) tafel curve of coating 20% AL_2O_3

Tables (12, 13) show the corrosion rates obtained by using the Tafel curve for 6 models. The lowest corrosion rate for the fourth model (10%) but when the percentage of alumina increases, the corrosion rates begin to rise.

Table (12) corrosion data.

Percentage AL_2O_3	E (V)	I_{corr} (A/cm^2)	$-b_c$ (mv)	$+b_a$ (mv)
pure	-0.72747	1.6836E-05	807.5	154.43
coating	-0.55034	0.48082E-05	6032.3	322.81
C (5%)	-0.2014	1.8554E-06	1397.8	2775.5
D (10%)	-0.36118	2.4818E-07	508.8	172.8
E (15%)	-0.1412	1.6311E-05	1431.9	3151.3
H (20%)	-0.17178	1.8235E-06	749.54	3016.4

Table (13) show the corrosion rates using the Tafel curve

Percentage AL_2O_3	$C_{R\ mm/a}$	$C_{R\ mpy}$
Pure A (0%)	0.1975	0.0050165
Coating B(0%)	0.056407	0.0014327
C (5%)	0.021883	0.0005558
D (10%)	0.0029115	0.0000739
E (15%)	0.019135	0.0004860
H (20%)	0.021392	0.0005433

Table (14) below shows the amount of weight loss for the models buried under the soil for three months

Percentage AL_2O_3	Weight before buried (g)	Weight after buried (g)	Amount of weight loss (g)
Pure A (0%)	6.036	6.000	0.036
Coating B (0%)	8.380	8.367	0.013
C (5%)	7.825	7.820	0.005
D (10%)	6.935	6.926	0.009
E (15%)	7.217	7.203	0.014
H (20%)	7.576	7.560	0.016

Figures (21, 22) shows the sharp decrease in the corrosion curve and the similarity in the corrosion rate between the electrochemical reaction models and the burial models, where the corrosion rate for the electrochemical reaction is at its lowest value at 10%, while the lowest value for the burial models is at 5%.

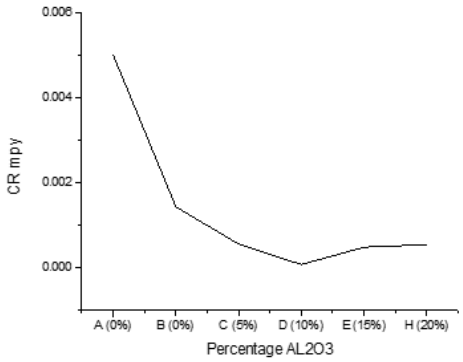

Figure - 23 - corrosion rate for the electrochemical reaction.

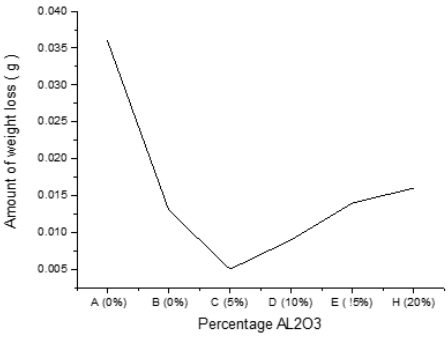

Figure - 24 - corrosion rates for the burial models.

4. Conclusions

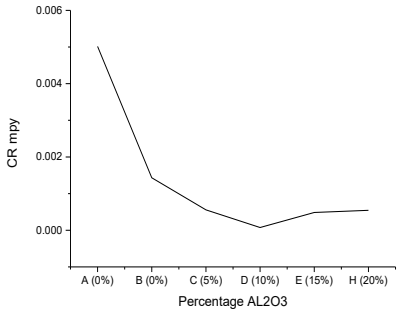

We conclude from this work the following:

1-All samples tested are to improve using the prepared coating compared to those without coating.

2-The corrosion resistance of samples treated with coating increases compared to those not treated.

3-The best samples were those using low percentages of coating supported by nano-aluminum oxide powder.

4-We note the convergence of the results between the method of burying samples in the soil with the electrochemical method are better in terms of their corrosion resistance for all samples.

Reference:

1. American Society for Testing and Materials. (2013). Standard Reference Test Method for Making Potentiodynamic Anodic Polarization Measurements (Designation: G5-13e1).

2. Bai, X., Tang, J., Gong, J., & Lü, X. (2017). Corrosion performance of Al–Al2O3 cold sprayed coatings on mild carbon steel pipe under thermal insulation. Chinese Journal of Chemical Engineering, 25, 533–539. https://doi.org/10.1016/j.cjche.2016.10.004

3. Banach, J. (2004). Liquid epoxy coatings for today's pipeline coating challenges. Northern Area Western Conference.

4. Beavers, J. A., & Thompson, N. G. (2006). External corrosion of oil and natural gas pipelines. In S. D. Cramer & B. S. Covino (Eds.), ASM Handbook: Corrosion: Environments and Industries (Vol. 13C, pp. 1015–1025). ASM International.

5. Bidder, S. H., & Bachelor, M. C. (2013). Impacts of water quality on residential water heating equipment. Pacific Northwest National Laboratory, Prepared for the U.S. Department of Energy, Contract DE-AC05-76RL01830.

6. Cantarelli, M. A., Pellerano, R. G., Marchevsky, E. J., & Camiña, J. M. (2008). Quality of honey from Argentina: Study of chemical composition and trace elements.

7. Cheng, Y. F. (2013). Stress corrosion cracking of pipelines (1st ed.). John Wiley & Sons.

8. Czupryński, A. (2017). Properties of Al2O3/TiO2 and ZrO2/CaO flame sprayed coatings. Spajanie Materiałów Konstrukcyjnych.

9. Czupryński, A., Tomiczek, B., Górka, J., & Adamiak, M. (2016). Testing of flame sprayed Al2O3 matrix coatings containing TiO2. Archives of Metallurgy and Materials.

10. Dehghanghadikolaei, A., Mohammadian, B., Namdari, N., & Fotovvati, B. (2018). Abrasive

machining techniques for biomedical device applications. Journal of Materials Science, 5, 1–11.

11. Derazkola, H. A., & Simchi, A. (2018). Effects of alumina nanoparticles on the microstructure, strength and wear resistance of poly(methyl methacrylate)-based nanocomposites prepared by friction stir processing. Journal of the Mechanical Behavior of Biomedical Materials, 79, 246–253.

12. Fu, A. Q., & Cheng, Y. F. (2010). Electrochemical polarization behavior of X70 steel in thin carbonate/bicarbonate solution layers trapped under a disbonded coating and its implication on pipeline SCC. Corrosion Science, 52, 2511–2518.

13. Ikechukwu, A. S., Obioma, E., & Ugochukwu, N. H. (2014). Studies on corrosion characteristics of carbon steel exposed to Na2CO3, Na2SO4 and different concentrations of NaCl solutions. International Journal of Engineering and Science (IJES), 3(10), 48–60.

14. Jameel, A. M., Kadhim, B. B., & Farhan, F. K. (2021). Improvement of corrosion protection of oil pipeline welding via adding tin disulfide nanoparticles. Al-Mustansiriyah Journal of Science, 32(4), 83–88.

15. Jia, R., Unsal, T., Xu, D., Lekbach, Y., & Gu, T. (2019). Microbiologically influenced corrosion and current mitigation strategies: A state-of-the-art review. International Biodeterioration & Biodegradation, 137, 42–58.

16. Kadhim, F. S. (2011). Investigation of carbon steel corrosion in water drilling mud. Modern Applied Science, 5(1), 224.

17. Mirza, M. M., Rasu, E., & Desilva, A. (2016). Influence of nano additives on protective coatings for oil pipelines of Oman. International Journal of Chemical Engineering and Applications, 7(4), 221–224.

18. Mousa, F. H., Mahdi, A. S., Kadhim, B. B., & Ali, A. M. (2019). Technological characteristics of perovskite solar cell windows using CdS–wurtzoid structure. In AIP Conference Proceedings (Vol. 2190, No. 1, p. 020032). AIP Publishing.

19. Noveiri, E., & Torfi, S. (n.d.). Nano coating application for corrosion reduction in oil and gas transmission pipe: A case study in south of Iran. International Conference on Advanced Materials Engineering, 15, Singapore.

20. Quej-Ake, L. M., Contreras, A., Liu, H. B., Alamilla, J. L., & Sosa, E. (2019). The effect of hydrodynamics and temperature on corrosion rate of API steels exposed to oilfield produced water. Anti-Corrosion Methods and Materials, 66, 101–114.

21. Sekunowo, O. I., Adeosun, S. O., & Lawal, G. I. (2013). Potentiostatic polarisation responses of mild steel in seawater and acid environments. International Journal of Scientific & Technology Research, 2(10), 139–145.

22. Sulaiman, Q. J., Al–Taie, A., & Hassan, D. M. (2014). Evaluation of sodium chloride and acidity effect on corrosion of buried carbon steel pipeline in Iraqi soil. Iraqi Journal of Chemical and Petroleum Engineering, 15(1), 1–8.

23. Szala, M., Dudek, A., Maruszczyk, A., Walczak, M., Chmiel, J., & Kowal, M. (2019). Effect of atmospheric plasma sprayed TiO2-10% NiAl cermet coating thickness on cavitation erosion, sliding and abrasive wear resistance. Acta Physica Polonica A, 136(2).

24. Usman, A. D., & Okoro, L. N. (2015). Mild steel corrosion in different oil types. International Journal of Scientific Research and Innovative Technology, 2(2).

25. World Steel Association. (2019). World steel in figures 2019. Brussels, Belgium. Retrieved from https://www.worldsteel.org/publications/infographics.html (Accessed on June 2, 2020).

26. Yu, T., Yan, M., Yu, L., Zhao, H. T., Sun, C., Yin, F., & Ke, E. (2019). Stress corrosion of pipeline steel under disbonded coating in a SRB-containing environment. Corrosion Science, 157, 518–530.